Exciton binding energies and diamagnetic shifts in semiconductor quantum wires and quantum dots

M. Bayer
Technische Physik, Universität Würzburg, Am Hubland, D-97074 Würzburg, Germany

S. N. Walck
Naval Research Laboratory, Washington, DC 20375

T. L. Reinecke
Technische Physik, Universität Würzburg, Am Hubland, D-97074 Würzburg, Germany and Naval Research Laboratory, Washington, DC 20375

A. Forchel
Technische Physik, Universität Würzburg, Am Hubland, D-97074 Würzburg, Germany

(Received 20 June 1997)

Systematic studies of the effects of confinement and reduced dimensionality on excitons in quantum wires and quantum dots have been made on systems with widely varying sizes. Diamagnetic shifts are obtained from low-intensity magnetophotoluminescence spectroscopy, and exciton binding energies are estimated using an anisotropic bulk exciton model. Modulated barrier and deep-etched $In_{0.10}Ga_{0.90}As/GaAs$ structures are used in order to study the dependence on the lateral potential offset. Calculations of the diamagnetic shifts and the binding energies are made using variational techniques, and are found to be in good agreement with experiment. For the sizes studied experimentally, the binding energies are found to be enhanced by up to four times the bulk value for wires, and by five times for dots. Further, confinement is found to have significant effects on the excitonic properties for structure sizes up to ten times the Bohr radius. [S0163-1829(98)01612-9]

I. INTRODUCTION

Excitonic effects play a central role in the optical properties of semiconductors. In semiconductor nanostructures the electron-hole interaction is enhanced by confinement, which increases the overlap of the electron and the hole wave functions. The electron-hole overlap is determined by the size of the nanostructures and by the height of the confining potentials. In addition, the overlap is enhanced by reducing the effective dimensionality of the system. Thus the binding energies are expected to increase in going from bulk to quantum wells, and further to quantum wires and quantum dots. In these structures excitonic effects are important both for the basic optical properties and for potential applications. In GaAs quantum wells, for example, excitons are prominent features in their optical properties at room temperature, although this is not the case in bulk.[1]

Excitonic effects are of importance in a variety of aspects of the behavior of low-dimensional systems including their nonlinear optical properties, time-dependent and transport properties, and exciton-exciton interactions. Here we are primarily interested in quantum wires and quantum dots. In an ideal one-dimensional system the exciton energy is divergent. In real quantum wires, however, this divergence is expected to be weakened, and the oscillator strength distributed among the interacting electron-hole states. In quantum dots a spatial separation of electron and hole is prevented by the three-dimensional geometric confinement. The exciton binding energy is the difference in energy between an electron-hole pair interacting by their mutual Coulomb attraction and an uncorrelated electron-hole pair. In order to understand excitonic effects quantitatively in realistic systems, it is necessary to understand the dependence of excitonic properties, particularly the binding energy, on the size, shape, and potential of structures.

Excitons in quantum wells have attracted considerable attention in recent years.[2] In addition, there have been extensive studies of excitonic transitions in microcrystals and related structures.[3] Theoretical studies of the effects of confinement and of decreased dimensionality on excitons have been made both for quantum wires[4–6] and quantum dots.[3,7–10] For quantum wires there have been few experimental studies, and they have been for structures of similar sizes.[11–14] In quantum dots it has often been difficult to obtain accurate, systematic values of exciton binding energies from spectroscopic data.[15]

In the present work we give the results of a systematic study of the effects of confinement and of dimensionality and also of lateral potential height on excitons in quantum wire and dot systems. Two different types of structures, each having a wide range of lateral sizes, are investigated. These structures differ with respect to the height of the lateral confinement, with the confinement being rather shallow for modulated barrier structures and very large for deep-etched structures. The diamagnetic shifts of the excitonic emission are measured in low excitation magnetophotoluminescence experiments, and are used to obtain exciton binding energies from an anisotropic bulk exciton model. The exciton binding energies are found to be enhanced substantially over the bulk value, and the effects of confinement on the exciton binding

energies are found to begin with sizes as large as ten times the Bohr radius. These effects are influenced by the heights of the confinement potentials. The binding energies and the diamagnetic shifts are shown to be in good agreement with detailed variational calculations for these structures.

The paper is organized as follows. In Sec. II A we give a short description of the samples and of the experimental setup, and in Sec. II B we present experimental results. In Sec. III we describe the theoretical approach used for the calculation of the binding energies and diamagnetic shifts. The experimental and theoretical results are compared and discussed in Sec. IV.

II. EXPERIMENT

A. Sample structures and experimental setup

$In_{0.10}Ga_{0.90}As/GaAs$ quantum wires and quantum dots of widely varying sizes are studied in the present experiments. These structures were fabricated by electron-beam lithography and wet chemical etching on an $In_{0.10}Ga_{0.90}As/GaAs$ quantum well with a width of 5 nm. Details of the fabrication process were given earlier.[16] In this way we obtained quantum wires with rectangular cross sections normal to the wire axis and quantum dots of cylindrical shapes in the quantum-well plane. The lateral sizes of the structures were determined using scanning electron microscopy. In the case of the wires we obtained structures with lateral widths less than 15 nm, and in case of the dots the smallest structure sizes were slightly more than 20 nm. Thus we were able to investigate wires and dots with sizes comparable to or larger than the exciton Bohr radius in the quasi-two-dimensional quantum well.

In order to investigate systems with varying lateral confinement heights, both free-standing deep-etched structures and effectively buried modulated barrier structures were fabricated. The heights of the lateral confinement potentials are drastically different in these two systems. In the case of modulated barrier structures, the total lateral confinement potential is about 25 meV, whereas in the case of deep-etched structures the confinement potential is given by the work function of the carriers, which is on the order of a few eV. Thus in deep-etched structures the lateral confinement potential is about two orders of magnitude greater than in buried structures. From optical spectroscopy and numerical calculations, a good understanding of the quantized single-particle states of the quantum wires and quantum dots has been obtained.[16,17]

The present experiments were performed in an optical split coil magnetocryostat ($B \leqslant 8$ T) at a temperature of $T = 2$ K. The measurements were performed in the Faraday configuration, that is, the magnetic field was aligned normal to the quantum-well plane (see the inset in Fig. 1). The samples were excited by a cw Ar^+ laser using very low excitation powers of less than 0.1 $W\ cm^{-2}$ in order to avoid high density effects. The luminescence was dispersed by a monochromator with a focal length of 0.6 m, and detected by a liquid-nitrogen-cooled Si charge-coupled device camera.

B. Photoluminescence studies

Figure 1 gives a series of low excitation photoluminescence spectra of large (453 nm) and small (28 nm) modulated barrier $In_{0.10}Ga_{0.90}As/GaAs$ dots for varying magnetic fields. In both cases a spectral line is observed which originates from ground-state exciton recombination in the dots. We made calculations of the energies of the single-particle states, from which we found that the experimental transition energies are systematically smaller than the calculated single-particle electron-hole transition energies. For this reason, and also because the optical excitation in the experiments is very low, we attribute the observed emission to excitonic recombination. As seen in Fig. 1, the lateral quantization shifts the emission of the small dots to higher energies by about 10 meV, as compared to the wide structures.

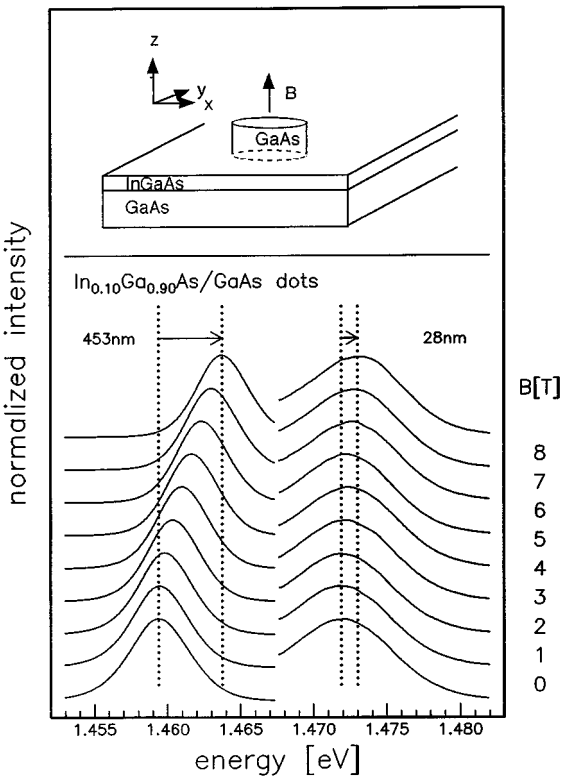

FIG. 1. Low excitation spectra of modulated barrier $In_{0.10}Ga_{0.90}As/GaAs$ dots with diameters of 453 (left) and 28 nm (right) for different magnetic field. The lines and arrows indicate the energy positions of the emission at $B = 0$ and 8 T for the two sizes. The inset gives a sketch of the modulated barrier structures.

With increasing magnetic field, the emission is continuously shifted to higher energies. At low magnetic fields this increase is weak, and it transforms into a stronger dependence at higher magnetic fields. The dotted lines in Fig. 1 indicate the positions of the spectral lines at $B = 0$ and 8 T. The relative shift is significantly greater for the larger dots, e.g., for 8 T it is 4.5 ± 0.2 meV for 453-nm dots and 1.3 ± 0.5 meV for 28-nm dots. The uncertainties in these values originate mainly from the inhomogeneous broadening of the luminescence due to size variations in the arrays of wires or dots.

A similar behavior is observed for modulated barrier quantum wires. Figure 2 shows the magnetic-field dependence of the luminescence transition energies of an unpatterned sample (bottom) compared to the energies of wires

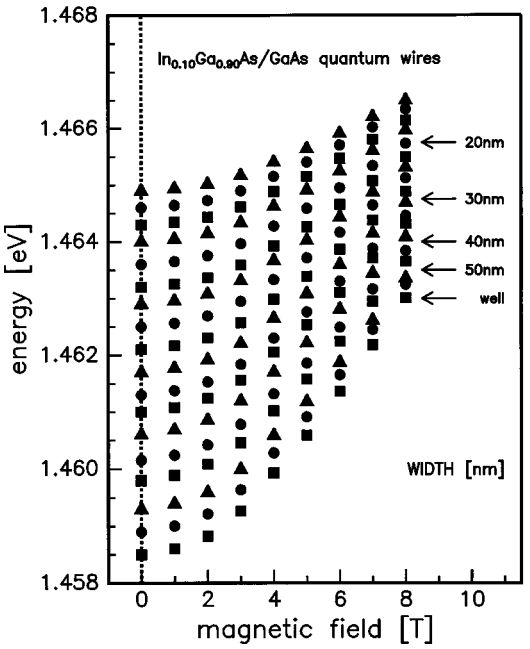

FIG. 2. Magnetic-field dependence of the ground-state exciton transition energies for modulated barrier $In_{0.10}Ga_{0.90}As/GaAs$ quantum wires with lateral sizes down to about 15 nm.

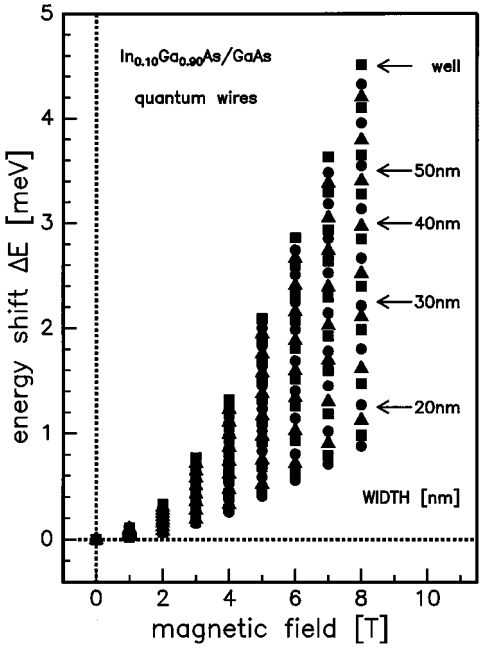

FIG. 3. Magnetic-field dependence of the shift of the ground-state exciton transition energies for deep-etched $In_{0.10}Ga_{0.90}As/GaAs$ quantum wires with lateral sizes down to about 15 nm.

with decreasing widths (from bottom to top). The position in energy of the exciton emission at $B=0$ is continuously shifted to higher energies with decreasing wire width due to the lateral quantization of the exciton. In addition, it is seen that the magnetic-field-induced shifts of the emission decrease systematically for decreasing wire width. In comparing these results for quantum wires with the corresponding results for the quantum dots above, we find that the decrease of the shift with decreasing size is greater for quantum dots than it is for quantum wires. For example, at 8 T and for wires with widths of ~ 30 nm, the shift is 2.5 ± 0.3 meV, whereas the shift for a dot with a diameter of 30 nm is 1.5 ± 0.5 meV.

Figure 3 shows the magnetic-field-induced shifts of the emission of deep-etched $In_{0.10}Ga_{0.90}As/GaAs$ quantum wires for magnetic fields up to 8 T. Qualitatively the same behavior is observed for them as for the modulated barrier wires. The diamagnetic shifts of the emission for large wires with sizes above 50 nm are similar to the shifts observed for the modulated barrier wires. Below a width of 50 nm, a strong decrease of the shift is again observed, but the magnitude of the decrease is larger than it is for the modulated barrier structures. For the smallest structures with widths of 15 nm, the shift of the emission up to 8 T is less than 1 meV in the case of deep-etched wires, while it is 1.5 meV in the case of the modulated barrier wires.

At low magnetic fields ($B \leqslant 4$ T) the shift of the transition energies is diamagnetic, $\Delta E=\gamma_2 B^2$, where γ_2 is the diamagnetic coefficient. From the diamagnetic coefficients we can obtain estimates for the exciton binding energies by comparing the measured diamagnetic shifts with those for a bulk system having anisotropic masses. This method was suggested in Ref. 12, and was shown to give good results by comparison to detailed calculations for the binding energies in Ref. 13. In this method the effect of the geometric confinement potential is represented approximately by the anisotropic deformation of the exciton wave function in a bulk model. The wave function is taken to be a hydrogeniclike ellipsoid of revolution, which is characterized by effective anisotropic Bohr radii a_B^i, $i=x,y,z$ parallel to its three principal axes or, equivalently, by direction-dependent reduced exciton masses μ_i, $i=x,y,z$ because $a_B^i \propto \mu_i^{-1}$. For such an asymmetric hydrogenic wave function, the diamagnetic shift is given by perturbation theory as[18]

$$\gamma_2=\frac{4\pi\hbar^2\varepsilon^2}{e^2\mu\mu_x\mu_y}, \quad \frac{1}{\mu}=\frac{1}{3}\left(\frac{1}{\mu_x}+\frac{1}{\mu_y}+\frac{1}{\mu_z}\right). \tag{1}$$

From the ratios of the experimentally observed diamagnetic coefficients for wires and dots to those of the reference quantum well, from Eq. (1) we obtain values of the in-plane reduced masses μ_x and μ_y. Here the magnetic field is along the growth direction (z) of the structures. For the quantum dots, μ_x is taken to be equal to μ_y, and for the quantum wires only the mass perpendicular to the wires is taken to vary due to the confinement. Then the exciton binding energy E_B is given by

$$E_B=\frac{e^4\mu}{32\pi^2\hbar^2\varepsilon^2}. \tag{2}$$

III. THEORY

We have made detailed variational calculations of the exciton diamagnetic shifts and of the exciton binding energies for the $In_{0.10}Ga_{0.90}As/GaAs$ quantum wires and quantum dots investigated in the present experiments. In order to calculate the diamagnetic coefficient, the exciton Hamiltonian is gen-

eralized to nonzero magnetic fields by the usual substitution $\mathbf{p}_i \rightarrow (\mathbf{p}_i + e_i \mathbf{A}_i)$, which gives

$$\mathcal{H} = \sum_{i=e,h} \left(\frac{1}{2m_i} (\mathbf{p}_i + e_i \mathbf{A}_i)^2 + V_c(\mathbf{r}_i) \right) - \frac{1}{4\pi\varepsilon\varepsilon_0} \cdot \frac{e^2}{|\mathbf{r}_e - \mathbf{r}_h|}. \quad (3)$$

Here the magnetic field $\mathbf{B}$ is given in terms of the vector potential $\mathbf{B} = \mathrm{curl}(\mathbf{A})$, and the confining potentials for electrons and holes are given by V_e and V_h, respectively. We found that the image charges at the vertical $In_{0.10}Ga_{0.90}As$-GaAs interfaces and at the lateral $In_{0.10}Ga_{0.90}As$ interfaces have negligible effects on the exciton properties, and thus we neglect them and use a single dielectric constant ε in Eq. (3). The interaction of the spin with the magnetic field is also neglected.

In the present quantum wire and quantum dot systems, the center-of-mass and relative coordinates no longer separate as they do in bulk and for quantum wells with perpendicular fields. In order to find the exciton states we first perform a canonical transformation on the Hamiltonian in Eq. (3). The canonical transformation is determined by four variational parameters. The exciton energy is expanded for small B and is minimized with respect to these parameters.

In order to calculate the exciton states and binding energies, we use the two parameter nonseparable functions

$$\psi_{\mathrm{exc}}(\mathbf{r}_e, \mathbf{r}_h) = \zeta_e(\cdots)\zeta_h(\cdots) \times \exp\{-\sqrt{\alpha[(x_h - x_e)^2 + (y_h - y_e)^2] + \beta(z_h - z_e)^2}\}. \quad (4)$$

Here $\zeta_e(\cdots)$ and $\zeta_h(\cdots)$ are the single-particle envelope functions for the quantized electron and hole states in the quantum wires and quantum dots in the absence of the electron-hole interaction.[16,17,19] For quantum dots (sketch in Fig. 1), ζ_i, $i = e,h$ are functions of (z_e, r_e) and (z_h, r_h), where z_i are along the heterostructure growth direction and r_i are the radial coordinates of the cylindrical dot. For quantum wires ζ_i are functions of (z_e, x_e) and (z_h, x_h), where x_i are perpendicular to the wire length. α and β are the variational parameters. The exciton energy is obtained by minimizing the expectation value of the Hamiltonian with respect to α and β:

$$\frac{\partial}{\partial \alpha, \beta} E_{\mathrm{exc}} = \frac{\partial}{\partial \alpha, \beta} \langle \Psi_{\mathrm{exc}} | \mathcal{H} | \Psi_{\mathrm{exc}} \rangle = 0.$$

The exciton binding energies are obtained by comparing the energy with the sum of the electron and hole single-particle energies for zero field. Studies of exciton binding energies in quantum wells using single-parameter ($\alpha = \beta$) nonseparable wavefunctions like that in Eq. (3) have shown that it gives accurate results for the binding energies for widely varying well widths.[2] Finally, the diamagnetic coefficients are given by

$$\gamma_2 = \lim_{B \rightarrow 0} \frac{dE_{\mathrm{exc}}(B)}{dB^2},$$

where $E_{\mathrm{exc}}(B)$ is the exciton energy as a function of the magnetic field.

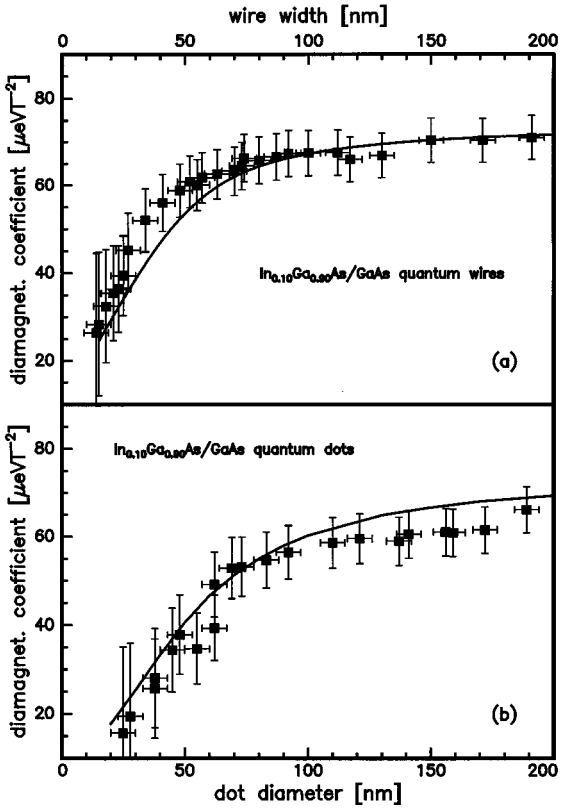

FIG. 4. Diamagnetic coefficients for modulated barrier $In_{0.10}Ga_{0.90}As$/GaAs quantum wires (a) and quantum dots (b) as functions of the lateral sizes of the structures. The symbols show the experimental results, and the lines give the results of the calculations.

The following material parameters were used in these calculations: For $In_{0.10}Ga_{0.90}As$ the electron and hole masses were taken to be $m_e = 0.0623$ and $m_h = 0.35$, and for GaAs they were $m_e = 0.0665$ and $m_h = 0.35$. The conduction- and valence-band offsets between $In_{0.10}Ga_{0.90}As$ and GaAs were taken to be $V_c = 69$ meV and $V_v = 37$ meV, respectively, and a dielectric constant ε of 13.0 was used for both semiconductors. This set of parameters gives a good description of the exciton binding energy and the diamagnetic shift for the quantum well, and allows us to study the effects of confinement in the quantum wires and quantum dots, which is the subject of interest here.

IV. DISCUSSION

A. Diamagnetic shifts

Figure 4 shows the diamagnetic coefficients for the modulated barrier quantum wires (a) and quantum dots (b). To determine these coefficients from the experimental results, a function proportional to B^2 was fitted to the observed exciton transition energies. This was done over a magnetic-field range from zero to some upper field strength B_{max}. The choice of B_{max} is given by the requirement that the cyclotron energy $\hbar\omega_c$ is clearly smaller than the excitonic Rydberg. In this case the quadratic dependence of the exciton energies on B is obtained. At higher magnetic fields ($\hbar\omega_c \gg Ryd$) the transition energies become more free-carrier-like. For small

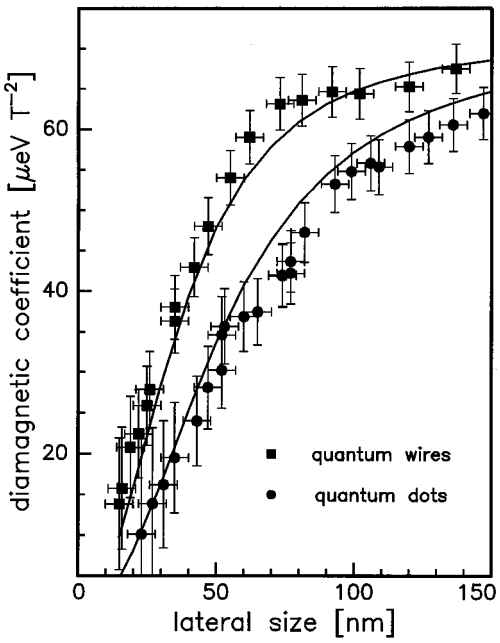

FIG. 5. Diamagnetic coefficients for deep-etched $In_{0.10}Ga_{0.90}As/GaAs$ quantum wires (a) and quantum dots (b) as functions of the lateral sizes of the structures. The symbols show the experimental results, and the lines give the results of the calculations.

fields, however, the shift of the excitonic emission is small, so there are experimental errors in determining γ_2. In order to obtain the most reliable results we take $B_{\max}$ to be 4 T. From our variational calculations we find that the linear terms in the exciton energy are small compared to the quadratic terms up to these fields.

From Fig. 4(a) it can be seen that in case of the quantum wires the diamagnetic coefficient remains almost constant, and equal to its value in the quasi-two-dimensional reference ($\sim 70\ \mu\text{eV T}^{-2}$) down to about a 50-nm wire width. Below this width γ_2 is observed to decrease. For wires of the smallest widths ~ 15 nm, γ_2 is reduced to less than $30\ \mu\text{eV T}^{-2}$. Qualitatively, the same behavior is observed for the quantum dots. γ_2 is nearly constant down to a certain dot diameter, after which it decreases. The decrease of γ_2 begins at a size of 100 nm in the case of the dots, as compared to 50 nm in the case of the wires. For the smallest dots with a diameter slightly smaller than 30 nm, γ_2 is already smaller than $20\ \mu\text{eV T}^{-2}$. The results of our calculations of the diamagnetic coefficient are also shown in Fig. 4 by solid lines. There it is seen that the data and the calculated results are in good agreement.

In the case of a quantum well in normal magnetic field, the diamagnetic coefficient can be related to the expectation value of the exciton radius in the well plane by

$$\gamma_2 = \frac{e^2}{8\mu} \langle x^2 + y^2 \rangle, \tag{5}$$

where $x = x_e - x_h$ and $y = y_e - y_h$. This result depends on the center-of-mass motion being separable from the relative motion, which arises from the translational invariance in the plane of the quantum well. In the cases of quantum wires and quantum dots, the motion is not translationally invariant in these directions, and the simple form in Eq. (5) no longer holds. In these cases the diamagnetic coefficient depends on the expectation values of the electron and hole coordinates in the plane separately, and more complicated forms than Eq. (5) have to be used for the diamagnetic shift of the exciton.[20]

In Fig. 5 we show the diamagnetic coefficients as functions of the lateral sizes for the deep-etched $In_{0.10}Ga_{0.90}As/GaAs$ wires (squares) and dots (circles). The solid lines again show the results of our calculations. The qualitative behavior in this case is similar to that observed for the modulated barrier structures. In particular, the decrease of γ_2 is significantly stronger for the quantum dots than for the quantum wires. However, for both the wires and dots the observed reduction of γ_2 in the deep-etched structures is greater than for the modulated barrier structures. For example, for 15-nm quantum wires we find a value of about $30\ \mu\text{eV T}^{-2}$ for the modulated barrier wires, and about $15\ \mu\text{eV T}^{-2}$ for deep-etched wires. For the smallest deep-etched quantum dots with a diameter slightly larger than 20 nm, γ_2 is decreased to about $10\ \mu\text{eV T}^{-2}$.

B. Exciton binding energies

The exciton binding energies are obtained from our experimental results for the diamagnetic coefficients by applying a model of an asymmetric bulk exciton. The binding energies for the modulated barrier quantum wires (squares) and dots (dots) are shown in Fig. 6. For the two-dimensional reference sample, we find a binding energy of 8.8 meV, which is, within the experimental error, identical to the value we obtain from the splitting of the $1s$ and the $2s$ excitons in

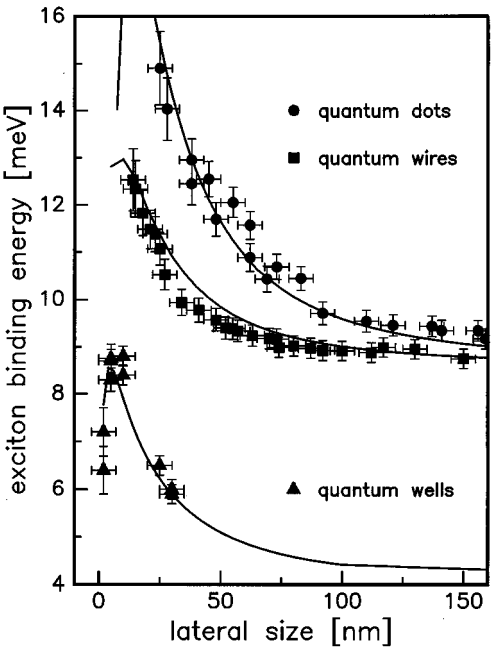

FIG. 6. Exciton binding energies as functions of the lateral structure size for the modulated barrier $In_{0.10}Ga_{0.90}As/GaAs$ quantum wires and quantum dots. The symbols show the experimental results, and the lines give the results of the calculations. The binding energies in $In_xGa_{1-x}As/GaAs$ quantum wells with In contents between 8% and 12% are also shown.

photoluminescence excitation studies on the quantum-well sample. In the case of quantum wires the binding energy remains to a good approximation equal to this value down to wire widths of about 50 nm. Below this size the binding energies increase continuously due to the lateral confinement, and for the smallest wires studied, with a width of 15 nm, a maximum binding energy of 12.5 meV is found. In the case of modulated barrier quantum dots, the increase starts for diameters of about 100 nm, and is greater than in case of the wires. For 30-nm-wide quantum dots the binding energy is 14 meV, in comparison to about 10 meV for 30-nm-wide quantum wires.

To obtain a broad picture of the dependence of the exciton binding energy on dimensionality, the results for $In_xGa_{1-x}As/GaAs$ quantum wells of varying widths also are shown in Fig. 6. The binding energy in the wires and dots for large sizes begins at the value for the 5-nm well. The In content of the quantum wells studied here varied between 8% and 12%. We note that we examined the dependence of the binding energy in quantum wells on the In content of $In_xGa_{1-x}As$ between 8% and 12%, which changes the barrier height modestly. We find both experimentally and theoretically that the dependence of the exciton binding energy on the In content is weak.

For bulk $In_{0.10}Ga_{0.90}As$ the exciton binding energy is 4.03 meV. For $In_{0.10}Ga_{0.90}As/GaAs$ quantum wells the binding energy can be increased by more than a factor of 2. The maximum value which can be obtained is about 9 meV, close to the value for the 5-nm-wide well which was the starting material for the fabrication of the quantum wires and quantum dots. The lateral patterning of this structure then gives rise to a further enhancement of the binding energy.

The results of our calculations for the exciton binding energies are shown as solid lines in Fig. 6, where it is seen that the agreement between theory and experiment is good for wells, wires, and dots. A noteworthy aspect of these results is that exciton binding energies are enhanced for structure sizes much larger than the exciton Bohr radius (~ 5 times for wires and ~ 10 times for dots). From our calculations we trace this behavior to the coupling of the electron and hole center-of-mass motion with their relative motion, both of which are confined in these structures. These results show the strong influence of the structure size and dimensionality on the exciton binding energies.

The exciton binding energies for the deep-etched $In_{0.10}Ga_{0.90}As/GaAs$ wires (squares) are shown in Fig. 7(a) together with the results for modulated barrier wires (circles). For wires above 50-nm width we find for both types of structures that the binding energies converge to that for the quasi-two-dimensional reference (~ 8.8 meV). Below 50-nm width, the increase of E_B is faster in the case of the deep-etched wires. For the smallest structures with widths of about 15 nm, E_B is already more than 15 meV in the case of the deep-etched structures, whereas it is about 12.5 meV in case of the modulated barrier structures. The results of the variational calculations for the binding energies are also shown in Fig. 7(a) by solid lines.

The calculated binding energies for the two kinds of structures show different behaviors for very small sizes. In the case of deep-etched structures the binding energies increase continuously with decreasing wire widths due to the strong lateral confinement potential. In the case of modulated barrier structures, in contrast, the binding energy reaches a maximum and then decreases for decreasing size. This arises because for small structures the single-particle states spread out beyond the barriers in the quantum well. When this occurs, the electron-hole overlap and the exciton binding decrease. This behavior is analogous to that for thin quantum wells which have a maximum in the binding energy versus well width (see Fig. 6). This turnover does not occur in deep-etched structures because of their large lateral potentials.

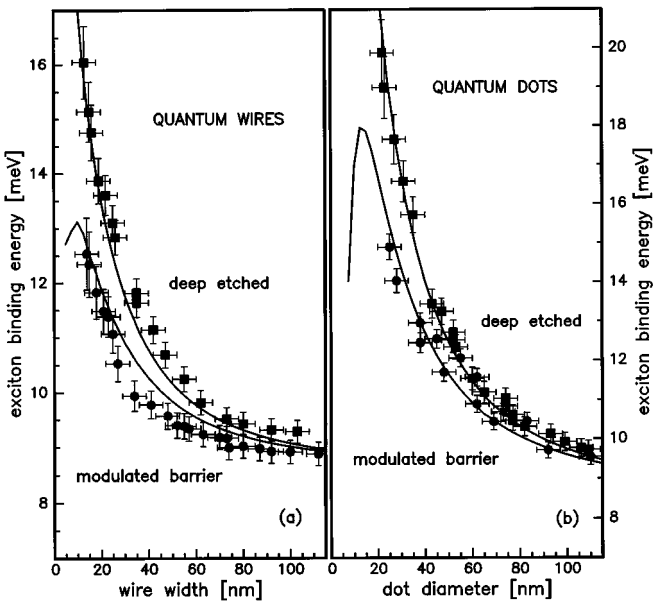

FIG. 7. (a) Comparison of the exciton binding energies as functions of the wire width for modulated barrier and deep-etched $In_{0.10}Ga_{0.90}As/GaAs$ quantum wires. The symbols show the experimental results, and the lines give the results of the calculations. (b) Comparison of the binding energies vs dot diameter for modulated barrier and deep-etched $In_{0.10}Ga_{0.90}As/GaAs$ quantum dots.

The experimental and theoretical results for the exciton binding energies of the deep-etched and modulated barrier quantum dots are shown in Fig. 7(b). For the smallest deep-etched quantum dots with diameters slightly less than 25 nm we find a binding energy of about 19 meV, which is more than two times the binding energy of the exciton in the 5-nm quantum well, and almost five times the corresponding bulk value. For dots with comparable sizes of about 30 nm, the binding energy is about 4 meV smaller in the buried structures than in the free-standing structures due to the smaller lateral confinement potential. We note that the exciton binding energy in the deep-etched dots can easily exceed the thermal energy at room temperature for structures with a diameter smaller than the exciton Bohr radius.

Exciton binding energies are functions of structure size and also of potential barriers. In the systems studied here the lateral potentials in the modulated barrier structures are quite small (tens of meV), and those in the deep etched structures are large (~ 5 eV). In this way we have been able to study the dependence of the binding energies on the lateral potentials. In Fig. 8 we show the dependence of the exciton binding energy in wires and dots as functions of the lateral potential offset for different sizes, (10, 27, and 80 nm). The

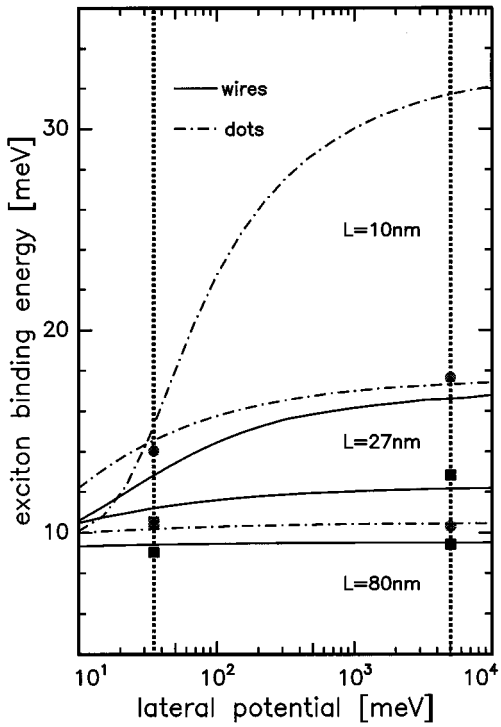

FIG. 8. Calculated exciton binding energies for 10, 27, and 80-nm-wide wires and dots as functions of the lateral confinement potential. The symbols give the experimental results for the modulated barrier and the deep-etched structures, for which the confinement potential heights are indicated by the dotted lines, respectively. For the 10-nm-wide structures, no experimental data exist.

data points shown there are for the modulated barrier and the deep-etched cases. The lines are results of our calculations for continuously varying potentials. The solid lines show the results for quantum wires, the dash-dotted lines those for quantum dots.

For the 80-nm-wide structures the binding energies are almost constant over the whole range of confinement potentials both for wires and dots; that is, we find that the dependence of the exciton binding energy on the lateral potential barrier is fairly weak in the regime of sizes for which the exciton wave function is well contained inside the nanostructures. On the other hand, with decreasing sizes the binding energies depend more strongly on the potential height. Then the binding energies increase fairly strongly for small confinement potentials, as can be seen for the 27-nm-wide structure and particularly for the 10-nm-wide structure. In contrast, for large potentials, i.e., for strong confinement of the wave function, the energies again show only a rather weak dependence on the potential.

For the 10-nm quantum dots we find for small potentials a crossing of their binding energy with the energy in the 10-nm-wide quantum wires, and also with that in the 27-nm-wide dots. The reason is that for small quantum dots the single-particle wave functions are pushed more and more out of the dot as the lateral confinement decreases. This leads to a comparatively stronger decrease of the binding energy.

V. SUMMARY

We made a systematic study of exciton binding energies in quantum wire and quantum dot systems. Experimental and theoretical results were obtained for widely varying sizes and potentials. In this way reliable results were obtained from which the physics of exciton confinement can be understood. For the sizes studied here experimentally, it was found that the binding energy can be enhanced by as much as a factor of 4 in wires and 5 in dots. Further, we found that the enhancement of the binding energy in these low-dimensional systems occurs for sizes as large as ten times the Bohr radius.

This clearly indicates that the effects of confinement on the exciton binding energies need to be taken into account for a quantitative understanding of optical phenomena in low-dimensional systems, even for structures of quite large sizes. This is the case, for example, when obtaining information about the geometry and potentials of the structures from their optical properties, as well as in studying such phenomena as optical nonlinearities, time-dependent and transport properties, and exciton-exciton interactions.

ACKNOWLEDGMENTS

T.L.R. gratefully acknowledges the financial support of the Alexander von Humboldt Foundation and the hospitality of the Max Planck Institute, Stuttgart. The financial support of the State of Bavaria and of the U.S. Office of Naval Research is gratefully acknowledged.

[1] See, for example, R. C. Miller and D. A. Kleinman, J. Lumin. **30**, 520 (1985).

[2] See, for example, R. C. Miller *et al.*, Phys. Rev. B **24**, 1134 (1981); G. Bastard *et al.*, *ibid.* **26**, 1974 (1982); R. L. Greene *et al.*, *ibid.* **29**, 1807 (1983).

[3] For a review of the investigation of exciton states in microcrystals see, for example, the comprehensive descriptions in U. Woggon, *Optical Properties of Semiconductor Quantum Dots* (Springer-Verlag, Berlin, 1997); A. D. Yoffe, Adv. Phys. **42**, 173 (1993).

[4] M. H. Degani and Oscar Hipólito, Phys. Rev. B **35**, 9345 (1987).

[5] J. W. Brown and H. N. Spector, Phys. Rev. B **35**, 3009 (1987).

[6] S. Christol, P. Lefevbre, and H. Mathieu, J. Appl. Phys. **74**, 5626 (1992).

[7] G. W. Bryant, Phys. Rev. B **37**, 8763 (1988).

[8] T. Takagahara, Phys. Rev. B **39**, 10 206 (1989); **47**, 4569 (1993).

[9] S. LeGoff and B. Stébé, Phys. Rev. B **47**, 1383 (1993).

[10] S. Jaziri, G. Bastard, and R. Bennaceur, Semicond. Sci. Technol. **8**, 670 (1993).

[11] M. Kohl, D. Heitmann, P. Grambow, and K. Ploog, Phys. Rev. Lett. **63**, 2124 (1994).

[12] Y. Naganume, Y. Arakawa, S. Tsukamoto, M. Nishioka, S. Sasaki, and N. Miura, Phys. Rev. Lett. **69**, 2963 (1994).

[13] R. Rinaldi, R. Cingolani, M. Lepore, M. Ferrara, J. M. Catalano, F. Rossi, L. Rota, E. Molinari, P. Lugli, U. Marti, D. Martin, F. Morier-Gemoud, P. Ruterana, and F. K. Reinhart, Phys. Rev. Lett. **73**, 2899 (1994).

[14] T. Someya, H. Akiyama, and H. Sakaki, Phys. Rev. Lett. **74**, 3664 (1995); **76**, 2965 (1996).
[15] Y. Nagamune, M. Nishioka, S. Tsukamoto, and Y. Arakawa, Appl. Phys. Lett. **64**, 2495 (1994).
[16] Ch. Gréus, L. Butov, F. Daiminger, A. Forchel, P. A. Knipp, and T. L. Reinecke, Phys. Rev. B **47**, 7626 (1993); Ch. Gréus, R. Spiegel, P. A. Knipp, T. L. Reinecke, F. Faller, and A. Forchel, *ibid.* **49**, 5753 (1994).
[17] M. Bayer, A. Forchel, I. E. Itskevich, T. L. Reinecke, P. A. Knipp, Ch. Gréus, R. Spiegel, and F. Faller, Phys. Rev. B **49**, 14 782 (1994); M. Bayer, A. Schmidt, A. Forchel, F. Faller, T. L. Reinecke, P. A. Knipp, A. A. Dremin, and V. D. Kulakovskii, Phys. Rev. Lett. **74**, 3439 (1995).
[18] S. Taguchi, T. Goto, M. Takeda, and G. Kido, J. Phys. Soc. Jpn. **57**, 3256 (1988).
[19] P. A. Knipp and T. L. Reinecke, Phys. Rev. B **54**, 1880 (1996).
[20] S. N. Walck and T. L. Reinecke, Phys. Rev. B (to be published).